

Single Breath-hold Abdominal T₁ Mapping using 3-D Cartesian Sampling and Spatiotemporally Constrained Reconstruction

Felix Lugauer¹, Jens Wetzl¹, Christoph Forman², Manuel Schneider¹, Berthold Kiefer², Dominik Nickel², and Andreas Maier¹

¹Pattern Recognition Lab, Department of Computer Science, Friedrich-Alexander-Universität Erlangen-Nürnberg, Erlangen, Germany, ²MR Applications Predevelopment, Siemens Healthcare GmbH, Erlangen, Germany

Synopsis

Volumetric T₁ mapping in the abdomen is desirable for whole liver assessment of hepatic diseases. In case of breath-hold imaging, accurate but time-consuming methods that sample the relaxation curve (IR or Look-Locker) are restricted to few slices only. To address these limitations, sparse Cartesian sampling with spatiotemporal incoherence is utilized to render 3-D Look-Locker within a single breath-hold possible. We demonstrate feasibility in both phantom and in-vivo measurements. The proposed method shows high agreement with a 2-D reference acquisition and enables an accurate mapping for a wide T₁ range, including very low values due to its high temporal resolution.

Introduction

Abdominal T₁ mapping can help diagnosing and staging hepatic diseases such as liver cirrhosis¹. Yet, accurate methods that are based on sampling the relaxation curve are usually limited to a few slices in case of breath-hold imaging. Common 3-D techniques are often based on a variable-flip-angle approach, which is B₁ sensitive, even when complemented with an additional B₁ mapping acquisition and correction². Look-Locker sequences are considered more accurate albeit time-consuming, restricting volumetric Look-Locker to static imaging only³. Sparse sampling with incoherence in both space and time can alleviate this problem. To this end, an existing 3-D CINE sequence prototype^{4,5} was extended to support inversion pulses and FLASH contrast.

We investigate whether the increased signal of 3-D acquisitions in combination with a sparse spatiotemporally incoherent sampling of the relaxation curve in high temporal resolution can yield T₁ values in a wide range with high accuracy. To our knowledge, this is the first application of whole-liver T₁ mapping and 3-D Cartesian Look-Locker within a breath-hold. Experiments include both phantom and in-vivo measurements.

Materials and Methods

A Look-Locker T₁-mapping scheme with continuous sampling after an initial inversion pulse was used. We utilized a multi-TI CINE protocol with an IR-FLASH sequence featuring adiabatic inversion⁴. Time points in the reconstruction were assigned to contrasts after inversion pulses. For sufficiently high spatiotemporal sampling density, k-space segmentation with multiple inversions and therebetween a wait-time for free relaxation was introduced.

A variable-density spiral spokes pattern ensured Cartesian sampling with a high temporal resolution⁵ (~100ms), which allows to determine very low T₁ values. For improved k-space coverage, multiple spiral arms were sampled in each shot and the set of spokes was rotated successively by the golden angle per shot and TI (Figure 1). Time-resolved reconstructions were performed using a FISTA algorithm⁶, which incorporates wavelet regularization in both space and time domain. 40 iterations with spatial/temporal regularization weights of 0.0006/0.007 were used. T₁ maps were obtained using a phase-corrected multi-step parameter fitting utilizing a smoothed flip angle map.

A 3 T MR scanner (MAGNETOM Skyra, Siemens Healthcare, Erlangen, Germany) was used for all experiments. An 18-channel body coil was used for volunteers, a 20-channel head coil for phantom experiments. Reconstructions were compared against 2-D multi-slice reference measurements of a prototypical LL sequence by means of ROI mean and standard deviation:

In-vivo: axial slices from a 6-slice 2-D acquisition were compared against corresponding slices in 3-D

Phantom: assessment based on the T₁-array of the NIST phantom⁷

3-D imaging parameters: FoV = 365x255x150mm³, matrix = 160x94x30, TR = 2.4ms, TE = 1ms, flip-angle = 6°, bandwidth = 1563Hz/Px, 19 TIs, ΔTI = 102ms, net acceleration = 15.4, acquisition window = 2s, wait time = 3.8s, 4 inversions.

2-D imaging parameters: FoV = 380x308mm², matrix size = 192x125 (1mm² interpolated), slice thickness = 5mm, TR = 3ms, TE = 1.3ms, flip-angle = 8°, bandwidth = 1530 Hz/px, 16 TIs, ΔTI = 225ms (2x acceleration), scan time = 22.8s (6 slices).

Results and Discussion

The 3-D+t image reconstructions took less than a minute using the scanner graphics hardware while T_1 mapping on the CPU (not parallelized) required 5–10s per slice. In-vivo results in Figure 2 show axial slices and a coronal reformation from the 3-D acquisition (A-C) in comparison to the 2-D reference (D,E). Figure 3 illustrates the signal recovery of the 3-D and 2-D acquisition in comparison. Labeled ROIs used for the in-vivo quantitative evaluation, which is presented in Table 1, are shown. Table 2 summarizes the results of the phantom evaluation.

Average hepatic T_1 values of 799 ± 32 and 810 ± 44 ms between the 2-D reference and 3-D show very high agreement in vivo. The phantom comparison shows excellent agreement with reference values for both methods in a wide range. Yet, only the 3-D acquisition with its short ΔT_1 , allowed determining phantom tubes with T_1 values as low as 60ms accurately. While the visual appearance between 2-D and 3-D is quite different due to image resolution, the 3-D acquisition, despite high acceleration, is hardly affected by artifacts and allows delineating most vessels and anatomical structures.

Conclusion

The feasibility of a 3-D Look-Locker acquisition for abdominal T_1 mapping within a single breath-hold was demonstrated. Utilizing an efficient reconstruction framework for spatiotemporal sparsity, our method enables whole-liver mapping with a $2.3\times 2.3\times 5\text{mm}^3$ resolution in 23s. Excellent agreement with a 2-D reference was shown for volunteer and phantom data for a wide T_1 range of 60–2000 ms. Additionally, the spatiotemporal sparsity enables the usage of very short ΔT_1 s making an accurate mapping of very low T_1 values feasible. Future works aims at improving scan efficiency.

Acknowledgements

This work was partly supported by the Research Training Group 1773 “Heterogeneous Image Systems”, funded by the German Research Foundation (DFG).

References

- [1] Haimerl M, Verloh N, Zeman F, et al. *Assessment of Clinical Signs of Liver Cirrhosis Using T_1 Mapping on Gd-EOB-DTPA-Enhanced 3T MRI*. PLoS ONE. 2014;8(12):e85658
- [2] Deoni S. *High-resolution T_1 mapping of the brain at 3T with driven equilibrium single pulse observation of T_1 with high-speed incorporation of RF field inhomogeneities (DESPO1-HIFI)*. J Magn Reson Imaging. 2007;26(4):1106-1111
- [3] Henderson E, McKinnon G, Lee, TY, et al. *A Fast 3D Look-Locker Method for Volumetric T_1* . Mapping Magn Reson Imaging 1999;17(8):1163-1171
- [4] Stalder AF, Speier P, Zenge M, et al. *Cardiac Multi-Contrast CINE: Real-Time Inversion-Recovery Balanced Steady-State Free Precession Imaging with Compressed-Sensing and Motion-Propagation*. In: Proceedings of the 22nd Annual Meeting of ISMRM. 2014.#431
- [5] Wetzl J, Lugauer F, Schmidt M, et al. *Free-Breathing, Self-Navigated Isotropic 3-D CINE Imaging of the Whole Heart Using Cartesian Sampling*. In: Proceedings of the 24th Annual Meeting of ISMRM. 2016.#411
- [6] Liu J, Rapin J, Chang T, et al. *Dynamic Cardiac MRI Reconstruction with Weighted Redundant Haar Wavelets*. In: Proceedings of the 20th Annual Meeting of ISMRM. 2012.#178
- [7] Keenan K, Stupic K, Boss M, et al. *Multi-Site, Multi-Vendor Comparison of T_1 Measurement Using ISMRM/NIST System Phantom*. In: Proceedings of the 24th Annual Meeting of ISMRM. 2016.#3290

Figures

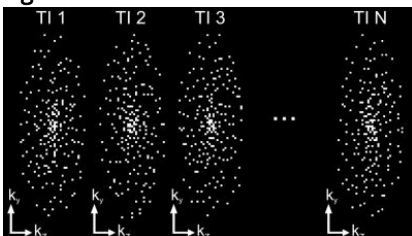


Figure 1: Incoherent sampling in space and time was implemented by a Cartesian spiral spokes pattern with variable density⁵. A golden angle rotation of subsequently generated spiral arms as well as jittering of oversampled positions targets good k-space coverage.

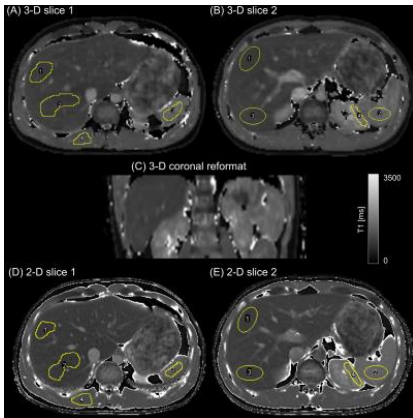


Figure 2: In-vivo comparison of a 3-D whole liver acquisition ($2.3 \times 2.3 \times 5 \text{ mm}^3$ resolution) against two 2-D reference acquisitions (1 mm^2 interpolated resolution) in two selected slices (A,B vs. D,E). The 3-D acquisition enables volumetric processing such as coronal reformation (C). Further shown are labeled ROIs, which are used for the quantitative evaluation.

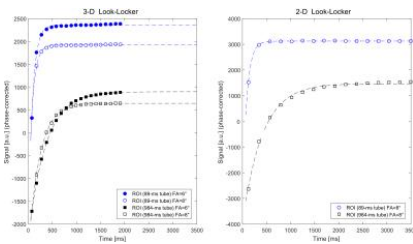


Figure 3: Exemplary recovery curves (effective T_1) for the 3-D Look-Locker acquisition (left) and the 2-D reference acquisition (right) for the phantom tubes⁷ $T1-3$ and $T1-10$. Unfilled markers mark the signal over time for a flip angle of 8° while filled markers correspond to a flip angle of 6° (3-D only). Dashed lines denote fits to the data. Note how the recovery plateaus earlier for the volumetric case, dependent on flip angle and TR. Further, the short ΔT_1 of the 3-D acquisitions is advantageous to capture the high dynamics in case of rapid relaxation.

Method	ROI 1 mean \pm SD	ROI 2 mean \pm SD	ROI 3 mean \pm SD	ROI 4 mean \pm SD
3-D slice1	812 \pm 36	798 \pm 54	1352 \pm 80	1048 \pm 49
3-D slice2	784 \pm 25	1346 \pm 83	846 \pm 50	1516 \pm 136
2-D slice1	784 \pm 30	761 \pm 37	1233 \pm 58	1029 \pm 40
2-D slice2	620 \pm 23	1346 \pm 51	831 \pm 37	1489 \pm 108

Table 1: In-vivo quantitative comparison based on ROI mean and standard deviation (SD) between the 2-D reference and 3-D Look-Locker acquisition.

Sample Name	Nominal values of "T1 array" at 3 T	LL 2-D: mean \pm SD (rel. error)	LL 3-D: mean \pm SD (rel. error)
T1-1	1080	2141 \pm 18 (8%)	2080 \pm 86 (5%)
T1-2	1050	1613 \pm 17 (4%)	1464 \pm 18 (1%)
T1-3	964	1099 \pm 17 (2%)	1009 \pm 20 (2%)
T1-4	768	728 \pm 8 (5%)	730 \pm 14 (3%)
T1-5	487	513 \pm 8 (5%)	500 \pm 15 (1%)
T1-6	392	360 \pm 12 (3%)	345 \pm 15 (5%)
T1-7	247	269 \pm 4 (5%)	231 \pm 8 (4%)
T1-8	178	180 \pm 3 (3%)	175 \pm 8 (5%)
T1-9	126	127 \pm 3 (1%)	127 \pm 4 (3%)
T1-10	89	93 \pm 4 (4%)	87 \pm 3 (3%)
T1-11	67	66 \pm 10 (16%)	62 \pm 4 (2%)
T1-12	45	413 \pm 88 (850%)	62 \pm 7 (16%)

Table 2: NIST phantom⁷ quantitative ROI comparison of the "T1 array" between the 2-D reference and 3-D acquisition.